NeuroImage 213 (2020) 116706

Contents lists available at ScienceDirect

NeuroImage

journal homepage: www.elsevier.com/locate/neuroimage

Multidimensional associations between cognition and connectome organization in temporal lobe epilepsy

Raúl Rodríguez-Cruces [a,b], Boris C. Bernhardt [b], Luis Concha [a,*]

[a] Universidad Nacional Autónoma de México, Instituto de Neurobiología, Querétaro, Querétaro, Mexico
[b] MICA Laboratory, Montreal Neurological Institute and Hospital, Montreal, Canada

ARTICLE INFO

Keywords:
Cognition
Connectome
Epilepsy
Multivariate
Network neuroscience

ABSTRACT

Objective: Temporal lobe epilepsy (TLE) is known to affect large-scale structural networks and cognitive function in multiple domains. The study of complex relations between structural network organization and cognition requires comprehensive analytical methods and a shift towards multivariate techniques. Here, we sought to identify multidimensional associations between cognitive performance and structural network topology in TLE.

Methods: We studied 34 drug-resistant adult TLE patients and 24 age- and sex-matched healthy controls. Participants underwent a comprehensive neurocognitive battery and multimodal MRI, allowing for large-scale connectomics, and morphological evaluation of subcortical and neocortical regions. Using canonical correlation analysis, we identified a multivariate mode that links cognitive performance to a brain structural network. Our approach was complemented by bootstrap-based hierarchical clustering to derive cognitive subtypes and associated patterns of macroscale connectome anomalies.

Results: Both methodologies provided converging evidence for a close coupling between cognitive impairments across multiple domains and large-scale structural network compromise. Cognitive classes presented with an increasing gradient of abnormalities (increasing cortical and subcortical atrophy and less efficient white matter connectome organization in patients with increasing degrees of cognitive impairments). Notably, network topology characterized cognitive performance better than morphometric measures did.

Conclusions: Our multivariate approach emphasized a close coupling of cognitive dysfunction and large-scale network anomalies in TLE. Our findings contribute to understand the complexity of structural connectivity regulating the heterogeneous cognitive deficits found in epilepsy.

1. Introduction

Temporal lobe epilepsy (TLE) is the most common drug-resistant epilepsy in adults and traditionally associated to mesiotemporal sclerosis, a lesion affecting the hippocampus and adjacent mesial structures (Blümcke et al., 2013). In addition to seizures, patients suffer from cognitive impairments that severely impact everyday functioning and wellbeing (Lin et al., 2012). In fact, TLE has traditionally been investigated by cognitive neuroscience as an important model to understand human memory and language dysfunction resulting from hippocampal damage (Hoppe et al., 2007).

Recent years have seen an evolution in our understanding of the cognitive landscape and structural compromise in TLE, fostered by an increasing administration of comprehensive neurocognitive phenotyping batteries and the advent of high-resolution and multimodal neuroimaging (Dabbs et al., 2009; Hermann et al., 2007). At the level of cognitive function, TLE is now recognized to perturb multiple domains not limited to memory and language processing (Helmstaedter and Elger, 2009; Hermann et al., 2007) These findings are paralleled by mounting neuroimaging evidence suggesting diffuse grey and white matter abnormalities beyond the mesial temporal lobe, affecting a distributed network of cortical and subcortical structures as well as their connections (Bonilha et al., 2013; Lin et al., 2007; Whelan et al., 2018). While some studies have shown compromise of both white and grey matter regions in TLE patients relative to the degree of cognitive dysfunction (Diehl et al., 2008; McDonald et al., 2014, 2008; Otte et al., 2012; Riley et al., 2010), we lack a comprehensive understanding on the association between the extent of network reorganization and overall cognitive performance.

* Corresponding author. Instituto de Neurobiología, Laboratory C-13, UNAM, Campus Juriquilla, Boulervard Juriquilla 3001, Juriquilla, Querétaro, C.P. 76230, Mexico.
E-mail addresses: raulrcruces@inb.unam.mx (R. Rodríguez-Cruces), boris.bernhardt@mcgill.ca (B.C. Bernhardt), lconcha@unam.mx (L. Concha).

https://doi.org/10.1016/j.neuroimage.2020.116706
Received 30 August 2019; Received in revised form 14 January 2020; Accepted 3 March 2020
Available online 6 March 2020

Associations between brain structure and cognitive performance are likely complex, particularly when multiple metrics are used for neuroanatomical profiling on the one hand, and cognitive phenotyping on the other hand. Inter-variable collinearities may furthermore challenge interpretability, and variables could lose their weight when tested individually. Multivariate analysis solves this problem by relating all measures in a single, compact model (McIntosh and Mišić, 2013). Although converging evidence suggest an association between network organization and cognitive impairments in TLE (Vaessen et al., 2012), virtually no previous research leveraged multivariate techniques to identify salient brain cognition associations in the condition. It remains unknown if there is a structural white matter network pattern associated with the cognitive decline seen in patients. We hypothesize that whole brain structural network abnormalities seen in TLE are closely associated with the heterogeneous cognitive performance.

We examined the interplay between multidimensional cognitive performance and structural network compromise in TLE patients and healthy controls. All participants underwent state-of-the-art multimodal magnetic resonance imaging (MRI) and neurocognitive assays. Multivariate Canonical Correlation Analysis (CCA) evaluated associations between multi-domain cognitive impairment and whole brain structural connectome reorganization. These models were complemented by unsupervised clustering techniques to identify cognitive subtypes in the TLE cohort, for which we identified morphological and network-based signatures. We leveraged bootstrap-based hierarchical clustering stability assessments as well as cross-validation techniques to strengthen robustness and replicability of discovered network substrates. Finally, we made all code and data related to our study openly available.

2. Materials and methods

2.1. Participants

The Ethics Committee of the Neurobiology Institute of the Universidad Nacional Autónoma de México approved this project (protocol code 019.H-RM) and written informed consent was obtained from all participants in the study according to the Declarations of Helsinki.

We recruited 34 adult ambulatory patients with drug-resistant TLE (Age = 29.7 ± 11.1 years; 22 females) and 24 age- and sex-matched healthy controls (Age = 32.8 ± 12.7 years; 18 females). Our cohort included 12 right TLE, 18 left TLE, and 4 bilateral TLE patients lateralized by seizure history and semiology, inter-ictal EEG recordings, and neuroimaging. All participants were right-handed native Spanish speakers. They did not have MRI contraindications nor other neurological comorbidities. Clinical features were obtained through a questionnaire-oriented interview upon referral (age at disease onset = 14.4 ± 9.3 years; seizure frequency per month = 4.2±+7.1, number of anti-epileptic drugs = 1.6 ± 0.6, 35.2% had a history of febrile seizures).

2.2. Data acquisition

2.2.1. Cognition

All participants underwent a comprehensive battery of cognitive tests: Wechsler Adult Intelligence Scale (WAIS-IV) and Wechsler Memory Scale (WMS-IV). We utilized the following index scores: auditory memory (AMI), visual memory (VMI), visual working memory (VWM), immediate memory (IMI), delayed memory (DMI), verbal comprehension (VCI), working memory (WMI), processing speed (PSI), and perceptual reasoning (PRI). Reported indices were normalized relative to a Mexican population and adjusted by age and education level. Details of the cognitive evaluation are described elsewhere (Rodríguez-Cruces et al., 2018).

2.2.2. Magnetic resonance imaging

Images were acquired with a 3 T Philips Achieva TX scanner with a 32-channel head coil. T1-weighted volumes (three-dimensional spoiled gradient echo) had a voxel resolution of 1 × 1x1 mm^3, repetition time (TR) of 8.1 ms, echo time (TE) of 3.7 ms, flip angle of 8°, and field of view (FOV) dimensions of 179 × 256 × 256 mm^3. Diffusion weighted images (DWI) were acquired with echo-planar imaging (EPI) and a 2 × 2x2 mm^3 voxel resolution, TR = 11.86 s and TE = 64.3 ms, and FOV = 256 × 256 × 100 mm^3. DWI were sensitized to 60 different diffusion gradient directions (b = 2000 s/mm^2); one b = 0 s/mm^2 volume was also acquired. An additional b = 0 s/mm^2 volume was obtained with reversed phase encoding polarity to account for geometric distortion corrections.

2.3. Image processing

2.3.1. Diffusion MRI processing

a) Diffusion weighted volumes (DWI) were denoised via data redundancy criteria from linear dimensionality reduction (Veraart et al., 2016), followed by non-uniform intensity normalization (Tustison et al., 2010). Reverse phase encoding from two b = 0 s/mm^2 volumes was used to estimate and correct for geometric distortions. DWI volumes were linearly registered to the b = 0 s/mm^2 images for motion correction and diffusion gradient vectors were rotated according to the transformation matrix.

b) Structural connectome parameterization. Using FreeSurfer v5.3.0, MRtrix 3.0, and FSL 5.0.6, we calculated individual structural connectivity matrices. Calculations were based on corrected DWI data and leveraged Spherical-deconvolution Informed Filtering of Tractograms, SIFT (Smith et al., 2013), with anatomically constrained tractography models, ACT (Smith et al., 2012). A total of 162 nodes were defined merging the cortical parcellation from the Destrieux Atlas and volBrain's subcortical segmentation (Supplementary Table 1). Whole brain tractography was first calculated using ACT with 20 million streamlines seeded from the grey-white matter interface, with maximum deviation angle of 22.5°, maximum length of 250 mm, minimum length of 10 mm. Tractograms were filtered with SIFT to 2 million streamlines (Fig. 1 top left). Connection weights between nodes (N_{SIFT}) were defined as the streamline count following SIFT (Smith et al., 2015a,b; Yeh et al., 2016, Fig. 1 top right), a procedure that has shown high reproducibility (Roine et al., 2019).

Connectivity matrices were analyzed using the *igraph R* package (igraph.org/r). We focused on path length, clustering coefficient, and degree centrality, the most widely used graph-theoretical parameters in the TLE literature (Bernhardt et al., 2015; Tavakol et al., 2019), also given that these measurements offer a compact description of global network topology and local connectivity embedding (Rubinov and Sporns, 2010). We computed the *clustering-coefficient* (*C*) as a measure of segregation, which provides information about the level of local connections in a network. The *characteristic path length (L)* measured network integration with short path lengths indicating globally efficient networks. Dijkstra's algorithm was used to calculate the inverse distance matrix and infinite path lengths were replaced with the maximum finite length. Finally, we calculated *degree centrality* (*k*) to characterize the relevance of the individual nodes. The current work was based on unthresholded, weighted networks. Of note, systematic evaluation of using different matrix thresholds showed high stability for thresholds above 60% of all possible connections (Supplementary Fig. 1).

2.3.2. Structural MRI processing

a) Hippocampal volumetry. T1-weighted volumes were processed using volBrain (volbrain.upv.es), which provides automated patch-based hippocampal and subcortical delineation with high accuracy in controls and TLE patients. Hippocampi were individually inspected by a trained rater, and hippocampal volumes were normalized by intracranial volume.

b) Cortical thickness analysis. Cortical thickness was measured for each participant using FreeSurfer v5.3.0. T1-weighted images were preprocessed through non-local-means denoising (Coupé et al., 2008) and N4 bias field correction (Tustison et al., 2010) prior to FreeSurfer segmentation. After processing, pial and white matter surfaces were visually

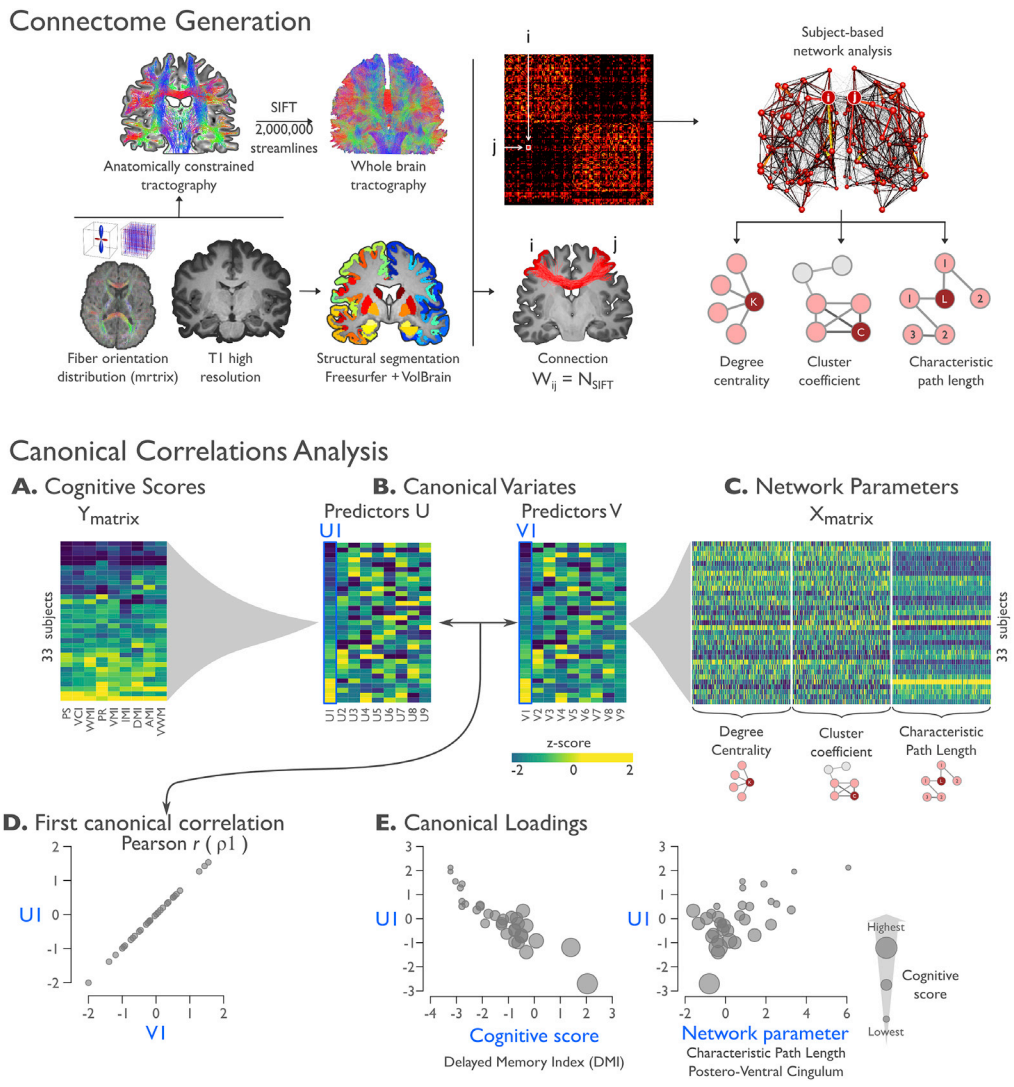

Fig. 1. Methods.

Connectome generation. Top left: Whole-brain connectomes were built using mrtrix, based on streamline counts derived from anatomically constrained tractography and spherical deconvolution informed filtering of tractograms (SIFT). Nodes were defined by merging the cortical segmentation of Destrieux Atlas and Volbrain's subcortical segmentation. Connection weight W_{ij} was defined as the streamline count between two nodes *ij* following SIFT. **Top right:** To study network topology, degree centrality, clustering coefficient, and characteristic path length were calculated based on the adjacency matrices. Cluster coefficient was calculated using the Onnela algorithm.

Multivariate analysis: canonical correlations. A. For each participant, the cognitive scores, excluding IQ were combined into matrix *Y*. Similarly, the nodal network measurements associated with a brain region were concatenated to a matrix *X* (**panel C**). **B.** The canonical variates are synthetic predictors (*V* and *U*) that maximize the correlations between the cognitive scores and the network parameters. **D.** The correlation between the first canonical variate U_1 and V_1 is referred as the first canonical correlation ρ1. **E.** The canonical loadings measure the linear correlation between an original variable of the cognitive scores Y_j or the network parameters X_j and a canonical variate.

inspected by a qualified trained rater and corrected if necessary. Individual surfaces were registered to a surface template with 20,484 surface points (fsaverage5) and a surface-based Gaussian diffusion filter with a full width at half maximum of 20 mm was applied, similar to our previous studies (Bernhardt et al., 2010).

2.4. Multivariate analyses

a) Regularized canonical correlation analysis. Canonical correlation analysis (CCA) assessed multivariate associations between cognitive scores and structural connectome measures (Fig. 1 bottom). Unlike principal components analysis (PCA) that reduces the number of variables in one set to components that emphasize variation in the data, CCA investigates the overall correlation between two multivariate datasets. CCA was recently employed in a large cohort of healthy adults to identify associations between neuroimaging-based connectivity measures on the one hand, and lifestyle, demographic, and psychometric measures on the other hand (Smith et al., 2015b).

First, we built a CCA to evaluate associations between connectome-derived parameters (k, C, and L) of all brain regions, and cognitive performance. Network parameters were concatenated into a one row vector per subject, resulting in a matrix X (subjects x network measurements). We excluded IQ because of its high correlation with all the remaining scores, resulting in a matrix Y (subjects x cognitive measures).

The main objective of CCA is to estimate canonical variates (U, V) that maximize the correlation between *network parameters*-X and *cognitive*

scores-Y (Fig. 1B bottom and Supplementary Fig. 2A). Resulting canonical variates can be ordered (U_1-U_n, V_1-V_n), with the first explaining the largest proportion of covariance among sets X–Y. Additionally, canonical loadings represent the relationship between an original variable and a canonical variate (Fig. 1E bottom).

As the number of subjects was less than the number of variables in both data sets, we included two regularization parameters for the covariance matrices X and Y (λ1 and λ2). Optimal parameters were estimated via leave-one-out cross-validation with recursive search on a two-dimensional surface grid. We directly searched for the maximum cross-validation value on the two-dimensional surface to obtain the optimal values for λ1 and λ2. These values are used to regularize the X and Y covariance matrices on the CCA model and solve the problem of $p \gg n$ and, to reduce overfitting due to the large number of variables. (see e.g., González et al., 2008 and Supplementary Fig. 2B).

Statistical significance of each CCA model was evaluated through permutation tests, randomly shuffling the rows of one of the input matrices (Y in this case) followed by running a permutation-based CCA. This built a null distribution of CCA results from which the associated p-values of the overall fit could be derived. Specifically, overall significance was determined by placing the original p-value into this distribution (see code in the repository for further details). Confidence intervals for CCA results were calculated using 10,000 bootstraps.

In addition to the main TLE-CCA model, we evaluated the following models to test for specificity: one with morphological measures (*i.e.,* volumetric of subcortical and cortical areas), one including only controls, one controlling matrix X and Y for hippocampal volume and mean cortical thickness, one controlling for age, duration of epilepsy and AED, and a full model that included network parameters, clinical features and volumes. The last two were performed to reveal clinical contributions above and beyond the structural effects on cognitive profiles.

Several analyses were employed to test for robustness of findings with respect to the nodal parcellation scheme on the CCA results. First, we evaluated our approach when combining the alternative Schaefer parcellation with 200 cortical nodes (Schaefer et al., 2017) and volBrain's subcortical nodes. We furthermore ran the CCA after compressing our network data based on a well-established functional community detection (Yeo et al., 2011, Supplementary Fig. 10). Finally, we applied dimensionality reduction of the X matrix with PCA prior to CCA analysis (Supplementary Fig. 11).

b) Stable cluster analysis for cognitive phenotypes. Clustering techniques have been suggested to capture heterogeneity in different clinical cohorts, and applied to cognitive variables in epileptic groups (Dabbs et al., 2009; Hermann et al., 2007). We clustered our TLE patients based on their cognitive scores to identify associations between cognition and connectome measures and assessed connectome-level comparisons between the clustered classes and healthy controls. Robust cognitive phenotypes were identified via unsupervised and bootstrap-supported analysis to identify maximally stable clusters (Fig. 2; Bellec et al., 2010). For each of the 10000 bootstrap iterations, we ran the k-means clustering algorithm with a set k ranging from 2 (minimum of 2 clusters) to 33 (N-1 clusters, N = number of subjects). During this process, we aggregated a stability matrix that collects the probability of each pair of subjects belonging to the same cluster (Fig. 1C and D). Stable clusters could thus be defined from this stability matrix, where clusters were formed by grouping participants that had a high probability of being clustered together irrespective of k.

c) Class difference analysis. Feature data, including hippocampal and subcortical volumes as well as cortical thickness, were z-scored based on controls and sorted into ipsilateral/contralateral relative to the seizure focus (Bernhardt et al., 2016; Liu et al., 2016). Bilateral patients (n = 4) were not sorted.

Clinical variables were compared between classes using ANOVAs followed by Tukey's post-hoc correction for multiple comparisons.

Topological nodal parameter (k, C, L) in the TLE group (see above for parameter sorting relative to the seizure focus) was compared to controls for each Class and represented as effect size (Cohen's D). For statistical comparison a node-level (ROI) *t*-test was performed for each TLE class compared to controls. Differences in nodal network parameters were corrected for multiple comparisons at a two-tailed false discovery rate (FDR) of q = 0.025.

Cortical thickness and subcortical volumes were compared to controls, and corrected with the mean cortical thickness for each subject. Surface-based analysis leveraged SurfStat for Matlab (Worsley et al., 2009). Effect size of the cortical thickness (Cohen's D) between group differences was calculated for each Class, and compared to controls at a vertex level using t-tests, and corrected for multiple comparisons with FDR, $q < 0.025$.

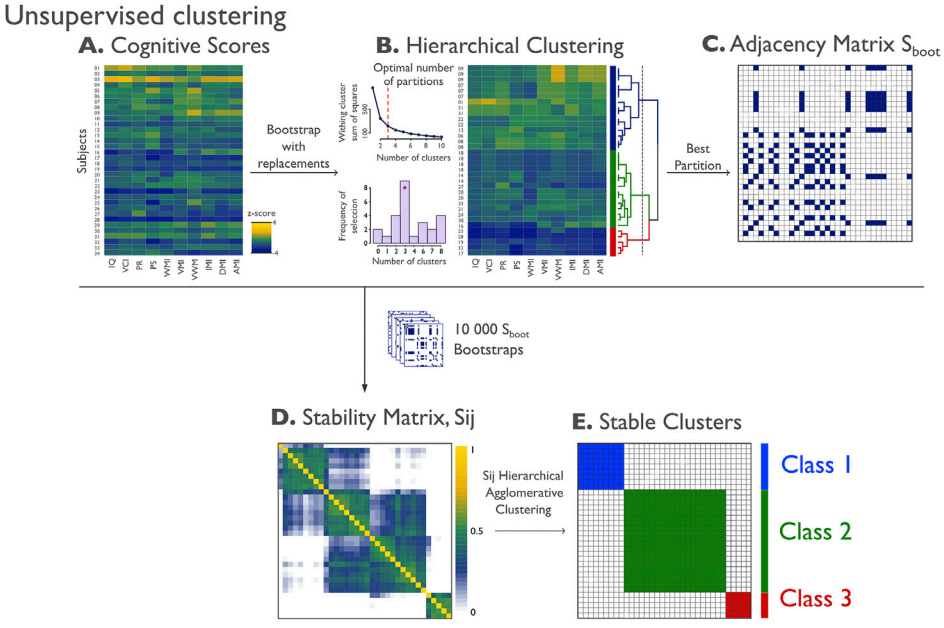

Fig. 2. Unsupervised clustering.
A) Cognitive features as z-scores with respect to controls are shown for each patient (rows). **B)** Example of a bootstrap with replacements realization with Ward D2 hierarchical agglomerative clustering. The optimal number of clusters (k) was determined from k = 2–33 **C)** Adjacency matrix of the optimal partition for each bootstrap S_{boot}, where $S_{boot}ij$ equals 1 if participants i and j belong to the same partition and 0 otherwise. **D)** After 10000 bootstraps, final stability matrix S_{ij} that represents the percentage of times a subject i was classified similarly to subject j. **E)** Hierarchical agglomerative clustering is performed over the stability matrix S_{ij}, clustering converges on a three subtype solution in our cohort.

3. Results

3.1. Multivariate association analyses

Canonical correlation analysis revealed one significant mode relating cognitive performance and structural connectome features in TLE (permutation-test $p < 0.05$; Fig. 3). Associated patterns of loadings showed that reduced cognitive scores related to reduced degree centrality and clustering, along with increased path length. Network loadings encompassed measures from cortical and subcortical regions and were high in both ipsilateral and contralateral regions. Specifically, longer path lengths related to lower cognitive scores in TLE, indicating associations between reduced global connectome efficiency and worse cognitive performance. Similarly, reduced degree centrality in bilateral superior frontal lobes, and precentral gyrus related to more marked cognitive dysfunction. Finally, clustering coefficient in ipsilateral parietal and middle frontal gyrus related to lower cognitive scores. When clinical and volume features were added to the CCA, results were consistent with the original model, adding negative loadings related years of study and volume of both hippocampi with lower cognitive scores (Supplementary Fig. 3).

Multivariate CCA between morphological measures and cognitive characteristics did not yield any significant associations in patients (Supplementary Fig. 4). Likewise, in our cohort no significant associations were found in healthy controls (Supplementary Fig. 5). Furthermore, the topological measures were independently associated with cognitive performance when controlling for hippocampal atrophy and cortical thickness (Supplementary Fig. 6). The first covariate describing relations between cognitive performance and network parameters was highly similar when additionally controlling for duration of epilepsy, age, and number of AED (Supplementary Fig. 7).

Degree centrality and clustering coefficient findings were consistent when using a different parcellation for the definition of cortical nodes (Supplementary Fig. 8). Although associations were slightly perturbed when removing subcortical nodes, they were still measurable (Supplementary Fig. 9). The first canonical variate of the Yeo communities showed a similar topological distribution of loadings to our main model (Supplementary Fig. 10). Taken together, these findings provide robust evidence for a close coupling of cognitive performance and whole brain white matter connectome topology in patients with temporal lobe epilepsy, suggesting a network level pattern underlying broad variations in cognitive function seen in these patients.

3.2. Cognitive classes

Bootstrap-based hierarchical clustering of cognitive profiles converged on three cognitive classes in our TLE cohort (Figs. 2E and 4A). Cognitive deficits showed an increasing gradient over the three classes, yet the pattern of these deficits was specific for each. Patients in Class 1 had cognitive scores within normal range, those in Class 2 showed mild impairment in memory-specific domains, and Class 3 displayed pronounced impairment across all domains, with prominent reduction of processing speed (Table 1). Notably, while there was heterogeneity within each Class (particularly Class 1, with some patients scoring higher than the average healthy control), the cognitive phenotypes that were identified by bootstrap-based hierarchical clustering stability assessments were very similar to those previously reported (Hermann et al., 2007).

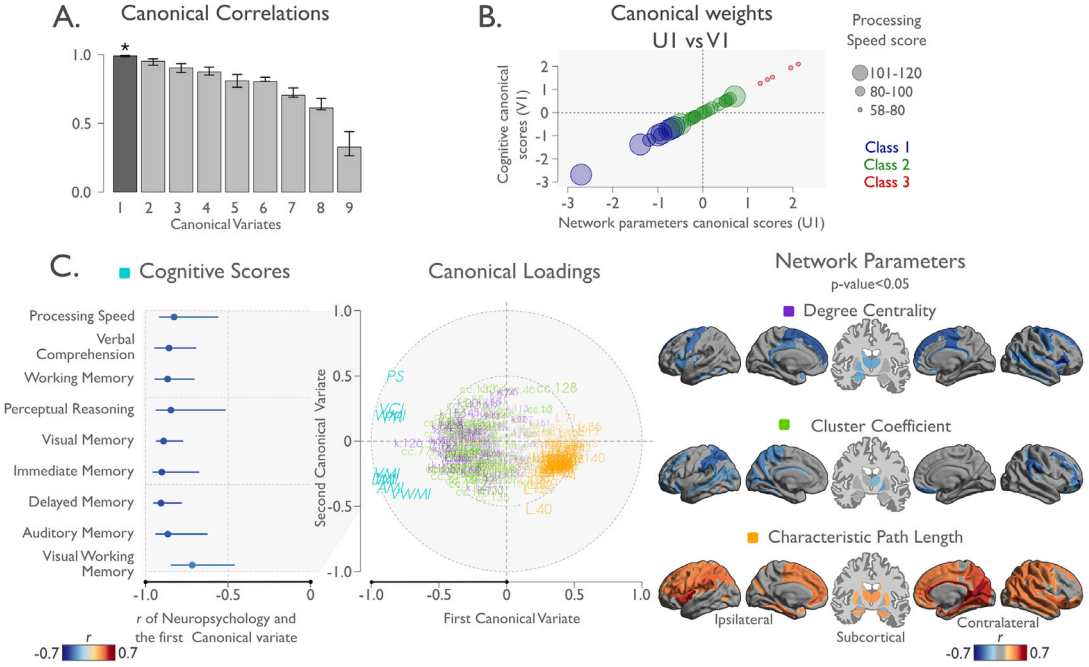

Fig. 3. Regularized canonical correlation solution.
A. Canonical correlations for each canonical variate, each with confidence interval and significance (* and darker grey indicate statistical significance). **B.** Scatterplot of the canonical weights assigned to the cognitive scores against the network parameter of the first canonical variate for each TLE patient (U1 versus V1). Processing speed score (PS) is shown as size of the circles, and color represents cognitive Class. **C.** Canonical cross-loadings of the first and second canonical variates for the cognitive scores and network parameters. Loadings are obtained by correlating each of the variables directly with a canonical variate. **C-Left** panel shows the correlation between each cognitive score and the first canonical variate. The lines represent the confidence interval over the first canonical variate (x-axis). **C-Middle** panel shows the cognitive scores and network loadings on the plane of the first and second canonical variates. Network loadings are shown with colors: Purple for degree, green for cluster coefficient and orange for characteristic path length. Cognitive loadings are shown in cyan: AMI-Auditory memory, VMI-visual memory, VWM-visual working memory, IMI-immediate memory, DMI-delayed memory, VCI-verbal comprehension, WMI-working memory, PS-processing speed and PR-perceptual reasoning. **C-Right** panel shows the significant network loadings of the first canonical variate, projected to the surface space and split by network measurement.

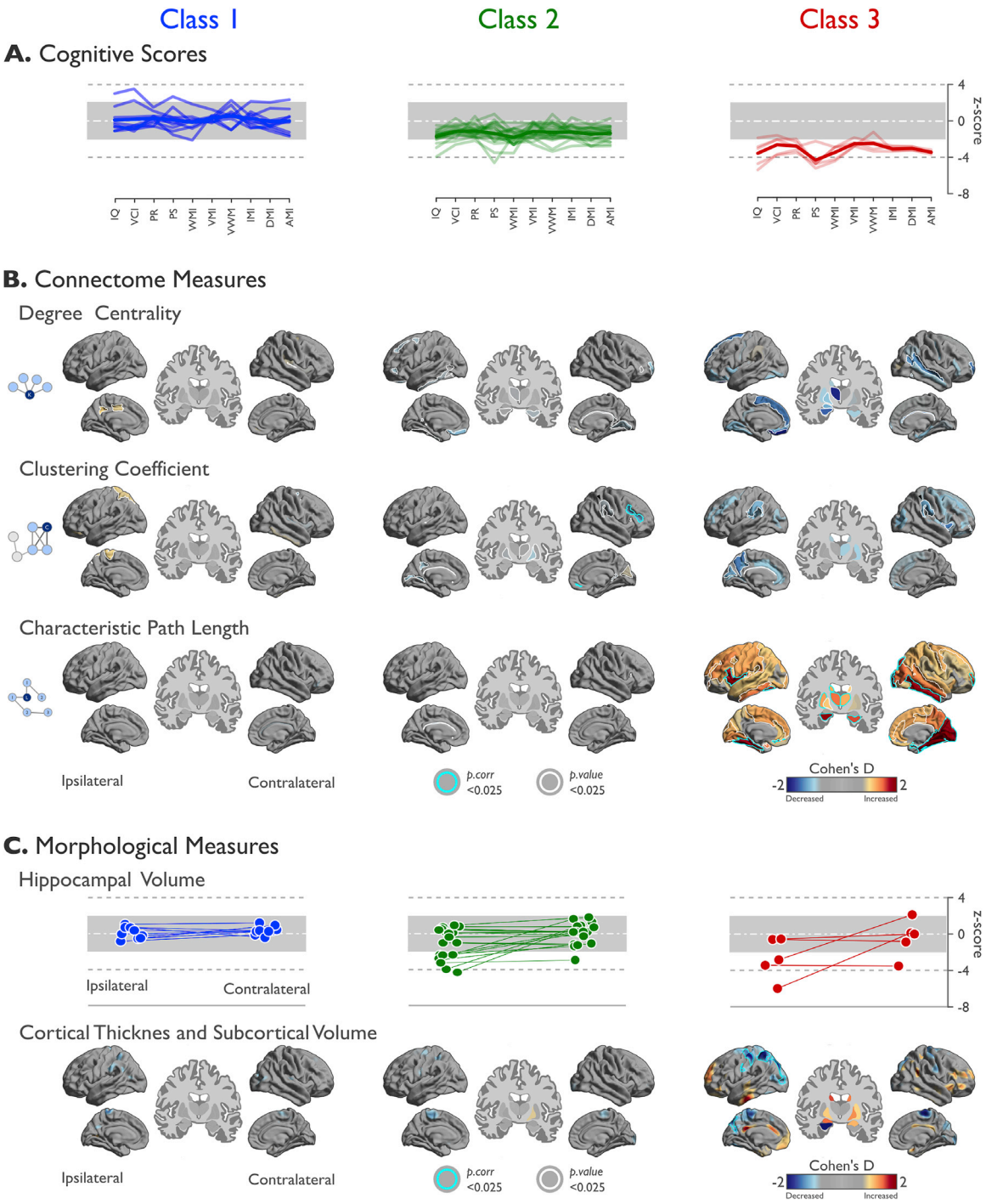

Fig. 4. Differences by cognitive class.
A. Cognitive scores for TLE patients by cognitive Class. Each patient is represented as a line indicating their normalized cognitive scores based on control, and the mean of each Class represented as a thick line. **B.** *Connectome measures.* For each metric, effect size (Cohen's D) of each Class compared to controls is projected over the surface. Significant differences corrected for multiple comparisons are outlined in cyan; white outlines represent uncorrected $p < 0.025$. **C.** *Morphological Measures.* Hippocampal volume is presented as z-score based on controls. Cortical thickness and subcortical volume are represented as Cohen's D compared to controls. Thickness is relative to the mean vertex value of each Class, while volume is the mean volume of each subcortical region.

Class 1 patients presented with older age of epilepsy onset, more years of education, and the shortest disease duration. Despite these clinical differences, findings were similar when controlling for age, duration of epilepsy, and number of antiepileptic drugs. Hippocampal sclerosis was less prevalent in Class 1 (33%) than Class 3 (80%, Table 1). White matter microstructure, as assessed with a tract-based spatial statistics framework, showed minimal abnormalities in Class 1, with an increasing amount of abnormal regions in Classes 2 and 3. Class 3 presents larger

Table 1
Clinical data by class. AED: number of antiepileptic drugs, HS, hippocampal sclerosis. Age, education, onset, duration and AEDs, degree centrality, path length, and cluster coefficient show as mean (standard deviation). *Significant difference compared to controls ($p_{adjusted} < 0.05$). Superscripts indicate significant difference with respect to the Class indicated by the number ($p_{adjusted} < 0.05$).

Clinical	Class 1	Class 2	Class 3
Number	9	20	5
HS *% presence*	**0.33***	**0.45***	**0.80***
Gender *% female*	0.56	0.75	0.40
Age *years*	28.7 (10.8)	30.9 (12.22)	26.4 (7)
Education *years*	14.3 (2.9)	12.4 (2.7)	**8.4 (1.3)*^{1,2}**
Age at onset *years*	19.2 (12.2)	13.8 (7.3)	8 (7.1)
Duration *years*	9.4 (8.7)	17.1 (14.7)	18.4 (8.3)
AED	1.3 (0.5)	1.7 (0.7)	1.6 (0.6)
Global network parameters			
Degree centrality	93.6 (3.6)	89.3 (5.6)	87.1 (4.3)
Path length x 10-4	31.2 (2.8)	31.3 (3.2)	**38.6 (11.6)*** ^{1,2}
Cluster coefficient	0.72 (0.01)	0.71 (0.01)	0.71 (0.01)
Cognitive performance			
Intelligence quotient	101.0 (13.7)	**82.8 (7.6)*^{1}**	**63.6 (14.7)*^{1,2}**
Verbal comprehension	100.7 (20.6)	**84.4 (7.8)*^{1}**	**64.6 (13.1)*^{1,2}**
Working memory	100.2 (11.6)	**82.3 (9.4)*^{1}**	**63.6 (8.8)*^{1,2}**
Perceptual reasoning	103.9 (8.9)	**86.5 (8.7)*^{1}**	**65.2 (7.8)*^{1,2}**
Processing speed	101.9 (10.4)	**90.4 (10.3)*^{1}**	**66.2 (9.6)*^{1,2}**
Auditory memory	97.1 (18.4)	**78.2 (11.0)*^{1}**	**49.2 (2.6)*^{1,2}**
Visual working memory	101.9 (7.7)	**76.3 (13.5)*^{1}**	**52.0 (7.3)*^{1,2}**
Immediate memory	99.1 (15.1)	**75.5 (11.6)*^{1}**	**44.6 (4.6)*^{1,2}**
Delayed memory	96.4 (16.6)	**73.7 (12.7)*^{1}**	**49.2 (3.3)*^{1,2}**

anomalies in white matter diffusion of major fascicles such as the bilateral anterior commissure, internal and external capsule, and a large proportion of the corpus callosum (Supplementary Fig. 12).

3.3. Connectome-level and morphological compromise across cognitive classes

Gradual network organization abnormalities were observed across Classes with most marked changes in Class 3, intermediate differences in Class 2, and only subtle changes in Class 1 (Fig. 4B). Although Class 1 presented with subtle increases of degree centrality and clustering coefficient relative to controls in cingulate and parietal cortices at uncorrected thresholds, these were not significant after correction for multiple comparisons. Class 2 showed decreased clustering in the contralateral suborbital sulcus and inferior frontal sulcus (p_{FDR}<0.025). At a connectome-wide level, Class 3 showed the most marked increases of characteristic path length (p_{FDR}<0.025), while Classes 1 and 2 were rather normal. In Class 3, path length increases were most marked in the lateral and medial temporal lobes in both hemispheres, the ipsilateral frontal and the contralateral occipital lobe.

Similar network parameter findings, we observed an increasing gradient of structural MRI changes from Class 1 (most similar to controls) to Class 3 (most abnormal, Fig. 4C). Hippocampal volumes in Class 1 were within the control range, while Class 2 and 3 had and increasing degrees of hippocampal atrophy. Cortical thinning was also most pronounced in Class 3, particularly in parietal areas ipsilateral to the focus.

A final integrative analysis examined associations between the rCCA and clustering solutions. This analysis revealed a tight relation between the first canonical variate (U1) with our clustering solution for all cognitive scores (Fig. 5). When we controlled our CCA model for hippocampal volume ipsilateral to the lesion and mean cortical thickness, the main canonical loadings were preserved, but the canonical weights lost their hierarchical relation with the cognitive metrics.

4. Discussion

The current work targeted the complex interplay between structural connectome reorganization and cognition in patients with drug-resistant temporal lobe epilepsy (TLE). Harnessing two complementary multivariate data science methodologies (*i.e.,* canonical correlation analysis and data-driven clustering), we observed converging evidence for a close associations between the overall degree of white matter network perturbations and multi-domain cognitive impairment in our patients. In particular, we found less efficient network organizations in patients with more marked cognitive difficulties. Notably, although complementary cortical thickness analysis revealed marked morphological anomalies in the same patient cohort, these measures were less closely associated to cognitive dysfunction than white matter connectome metrics. Furthermore, no significant associations were observed in controls.

Core to our data acquisition was a multi-domain cognitive phenotyping together with a whole-brain neuroimaging and connectomics paradigm. The use of a broad neuropsychological battery instead of restricted psychometric testing was motivated by prior observations suggesting that TLE impacts not only language and memory, but rather a diverse set of cognitive domains also including attentional and executive functioning (Dabbs et al., 2009; Hermann et al., 2007). Similarly, we employed hippocampal volumetry, cortical thickness analyses, as well as diffusion MRI connectomics to assess macroscale brain anomalies in both grey and white matter compartments. Prior histopathological and morphological studies have indeed suggested that although TLE is generally associated to mesiotemporal anomalies (Blümcke et al., 2013), it is rarely associated to a confined focal pathological substrate (Bernhardt et al., 2013; Blanc et al., 2011). Instead, an increasing number of MRI-based cortical thickness assessments and subcortical shape analyses have indicated a rather distributed structural compromise, often characterized by bilateral temporo-limbic as well as fronto-central atrophy (Bernhardt et al., 2010; Lin et al., 2007; Whelan et al., 2018). Similarly, a growing body of white matter tractographic analyses and network neuroscience work leveraging graph theoretical formalisms of structural connectomes suggested atypical white matter organization and microstructure not limited to the temporal lobe, but in a rather widespread topographic distribution radiating outwards from the mesiotemporal

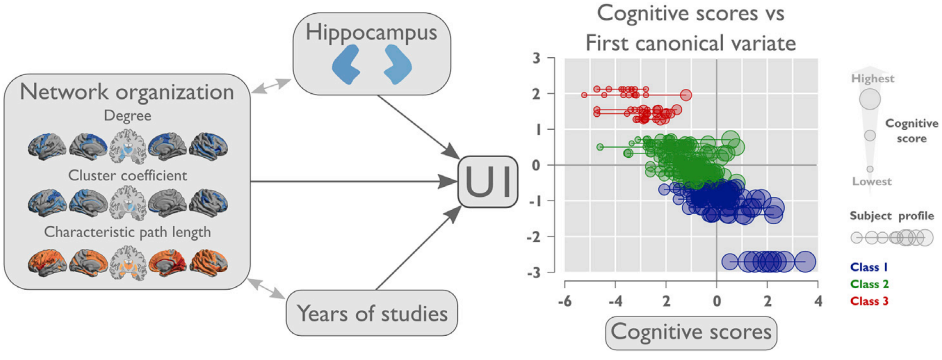

Fig. 5. Cognitive convergence.
Both methods used converge over the cognitive domain. The plot shows the relation between the first canonical variate and cognitive scores. Plot of the relation between the first canonical variate (U1) and all the cognitive scores, colored by class. Y-axis represents the value of the first canonical variate of the rCCA-TLE model for each subject, while on x axis we plot all the cognitive scores as z-score based on controls. Each subject's cognitive profile is shown as a horizontal line. The size of circles represents the score for each cognitive test. Individual cognitive tests are not distinguishable in this plot.

epicenter (Bonilha et al., 2013; Concha et al., 2005; Otte et al., 2012; Riley et al., 2010). Although these distributed abnormalities have been hypothesized to affect cognitive function (Lin et al., 2012), there are so far only sporadic systematic attempts to relate imaging measures to multi-domain cognitive phenotypes in TLE. In fact, among those studies associating structural anomalies and cognitive performance in TLE (Diehl et al., 2008; McDonald et al., 2014, 2008; Reyes et al., 2019; Riley et al., 2010; Rodríguez-Cruces et al., 2018), the majority has been rather selective, focusing on the relation between specific brain measures on the one hand, and particular cognitive domains on the other hand.

We harnessed multivariate associative techniques as well as bootstrap-based hierarchical clustering to integrate the broad panorama of cognitive phenotypes in TLE with connectomics and structural neuroimaging measures. The former class of models (McIntosh and Mišić, 2013), in our case a canonical correlation analysis (CCA), provides a set of sparse components capturing complex covariation patterns between network parameters and cognitive profiles. In healthy young adults, CCA has been used to identify gradual associations between functional connectome configurations and factors related to lifestyle, demographics and psychometric function, describing a positive-negative mode of covariation between observable behavior and self-report measures and functional connectome organization (Smith et al., 2015b). Similar methods were also leveraged to relate multimodal patterns of MRI and non-imaging measures using the UK Biobank database (Miller et al., 2016; Kernbach et al., 2018). In our TLE cohort, CCA revealed a consistent pattern of associations characterized by distributed increases in connectome path length related to reduced cognitive performance. Previous reports have shown similar increases of characteristic path length in this condition compared to controls, suggesting overall reduced global network efficiency (Bernhardt et al., 2011; Bonilha et al., 2012; Raj et al., 2010; Vaessen et al., 2012). Further elements of the brain-behavior covariation mode encompassed low frontal lobe clustering coefficient together with reduced parietal hubness in patients with reduced cognitive functions, potentially indicating a breakdown of frontal and parietal network segregation that may ultimately reflect network level consequences secondary to microstructural anomalies previously reported in these systems, notably axonal damage, myelin alteration, as well as reactive astrogliosis (Rodríguez-Cruces and Concha, 2015). As multivariate associative techniques like CCA can overfit, we incorporated several additional elements to ensure specificity and robustness. First, consistency was verified via cross-validation techniques, reducing potential hyper-optimization of within-sample associations at the expense to out-of-sample generalization. Second, we evaluated consistency of our CCA findings when using an alternative cortical parcellation scheme and when using an established community definition (Yeo et al., 2011), suggesting robustness of the observed brain-behavior associations with respect to nodal definition. Notably, including metrics of subcortical nodes revealed more extensive patterns of network abnormalities, in line with the known relevance of subcortical structures in capturing network-level pathology of TLE (Seidenberg et al., 2008). Finally, associations were more marked at the level of white matter connectomes than for grey matter morphometry, confirming overall a close association between white matter connectome architecture and cognitive phenotypes in the condition.

Further support for the consistency of the brain-behavior association in our patients was provided by data-driven clustering of the cognitive profiles, additionally supported in the current work using bootstrap based stability maximization (Bellec et al., 2010). Subtyping of epileptic patients based on cognitive profiles has previously been employed to identify a spectrum of cognitive function (Dabbs et al., 2009; Hermann et al., 2007; Reyes et al., 2019; Rodríguez-Cruces et al., 2018). The applied method converged on a three-class solution with gradual cognitive impairments and overall corresponding degrees of brain anomalies, assuring that cognitive impairment in TLE is indeed related to an increased load of white matter connectome reorganization, together with hippocampal and cortical grey matter atrophy. Integrative analyses confirmed that these discovered cognitive classes provide a different viewpoint on the dimensional multivariate mode of covariation seen via CCA (Fig. 5). Of note, the prevalence of hippocampal atrophy increased across the three cognitive classes, with the class showing the most marked cognitive dysfunction and connectome anomalies (*i.e.,* Class 3) also presenting the highest degree of hippocampal volume loss. Conversely, TLE laterality was similarly distributed across classes, potentially due to the broader range of domains evaluated in the current study than in work focusing on language and/or memory, which generally support more marked impairment in left compared to right TLE (Wieser and ILAE Commission on Neurosurgery of Epilepsy, 2004).

Several previous reports have related white matter abnormalities to cognitive deficits in TLE, with most previous studies focusing on specific white matter tracts and studying diffusion parameters derived from the diffusion tensor model, such as FA and MD (Diehl et al., 2008; McDonald et al., 2014, 2008; Riley et al., 2010; Rodríguez-Cruces et al., 2018; Reyes et al., 2019). While most reports have focused on TLE, some have also assessed other forms of epilepsy including genetic/idiopathic generalized syndromes (Niso et al., 2015). Despite heterogeneity in prior findings, the overall consensus of this work is that the overall degree of diffusion tensor abnormalities in specific tracts (or group of tracts) relates to the degree of cognitive decline seen in patients (Vaessen et al., 2012). Our work builds on this prior knowledge, addresses some conceptual and methodological issues, and provides a novel combination of several advanced methods in the context of TLE. First, in light of the widely-recognized shortcomings of the tensor model in quantifying structural connectivity (Qi et al., 2015; Jones et al., 2013, Maier-Hein, 2017), we leveraged an advanced CSD model, which allows tracking through areas of fiber crossing, which are pervasive throughout the human brain (Jeurissen et al., 2013). Furthermore, in contrast to basing our inference on the commonly used tensor derived metrics such as FA and MD, we used graph-theoretical parameterizations, which provide an integrative description of whole-brain network architecture and topology. Finally, instead of individually testing brain-behavior associations in preselected fiber bundles, we harnessed a multivariate statistical model (CCA), which provides an integrative whole-brain perspective on the association between cognitive burden and white matter damage. Prior applications have shown utility of such multivariate associative techniques in the context of healthy individuals (Smith et al., 2015b; Miller et al., 2016; Kernbach et al., 2018) and in neuropsychiatric populations (Kebets et al., 2019); here we provided a novel application of these methods to the study of brain-behavior relationships in epileptic populations. Notably, and in contrast to multiple prior studies, we evaluated multiple methodological choices in our work, including the effect of matrix thresholding, nodal definition, as well as associations to clinical and morphological confounds.

Our structural network findings showing topological anomalies in drug-resistant epilepsy results bear similarities with previous reports of altered functional connectivity in TLE that indicate reduced global efficiency in patients (Tracy and Doucet, 2015), and may partially resemble findings at the level of structural covariance suggestive of increased path length and clustering (Bernhardt et al., 2011, 2016; Yasuda et al., 2015; van Diessen et al., 2013). Although structural and functional connectivity cannot be equated, due to differential sensitivities of these techniques, both give interrelated approximations of macroscale networks (Mišić et al., 2015; Honey et al., 2009), and may tap into similar network mechanisms in disorders like TLE (Gleichgerrcht et al., 2015; Tavakol et al., 2019). Indeed, mirroring findings at the level of structural connectivity, prior functional connectivity analyses in TLE have suggested effects of seizure focus laterality (Barron et al., 2015, Lariviere et al., 2019, Morgan et al., 2015) and degrees of hippocampal pathology (Bernhardt et al., 2019). These findings are complemented by functional connectivity data based on intracranial recordings, suggesting associations between network properties and seizure evolution (Ponten et al., 2007; Khambhati et al., 2016).

Several factors need to be considered when interpreting our findings.

First, our sample size was modest and thus a potential limitation of the generalizability of our multivariate associative findings. Yet, in both our main and supporting analyses, we made several efforts to evaluate robustness with respect to methodological choices and across participant subsamples. Our approach furthermore resulted in the identification of cognitive subtypes in agreement with prior cognitive and morphometric studies (Hermann et al., 2007). Second, in light of known limitations of diffusion MRI in approximating structural networks in vivo (Jones et al., 2013; Qi et al., 2015, Maier-Hein, 2017), we adopted advanced methods to build structural connectomes. Specifically, we leveraged probabilistic tractography derived from constrained spherical deconvolution, instead of diffusion tensor networks, to track fibers even in regions of fiber crossing (Jeurissen et al., 2013). Moreover, prior work suggested high reproducibility when constrained spherical deconvolution derived-methods like SIFT with $\geq$1 M streamlines are used - algorithm parameters also chosen in the current study (Roine et al., 2019). Furthermore, although our study shows associations in patients that were not seen in controls, we still cannot establish specificity given the lack of disease controls in this work. Large-scale efforts such as enigma epilepsy, for example, have already begun to assess epilepsy-related anomalies to those in other disorders and it may be of relevance to also capitalize on these resources for brain-cognition studies (Whelan et al., 2018; Hatton et al., 2019). Finally, beyond these sample-specific and methodological considerations, the cross-sectional nature of our work cannot provide any insights into the causality between structural connectivity and cognition in TLE. Longitudinal designs, ideally at different disease stages, are required to disentangle the underlying directionality of effects (Caciagli, 2017; Bernhardt et al., 2010; Galovic et al., 2019).

In addition to the use of multivariate techniques and state-of-the-art connectomics and cognitive phenotyping, our findings are well anchored in overarching assumptions on the link between brain structure and function in healthy and diseased brains. Our findings encourage the use of multivariate methods and contribute to understand the complexity of structural connectivity regulating the heterogeneous cognitive deficits found in epilepsy.

Funding sources

This work was supported by a grant from the Mexican Council of Science and Technology (CONACYT, 181508, 1782); and from UNAM-DGAPA (IB201712, IG200117). Raúl Rodríguez-Cruces is a doctoral student from Programa de Doctorado en Ciencias Biomédicas, Universidad Nacional Autónoma de México (UNAM) and received fellowship 329866 from CONACYT. Imaging was performed at the National Laboratory for magnetic resonance imaging, which has received funding from CONACYT (grant numbers 232676, 251216, and 280283). Dr. Bernhardt acknowledges research funding from the National Sciences and Engineering Research Council of Canada (NSERC; Discovery-1304413), Canadian Institutes of Health Research (CIHR; FDN-154298), SickKids Foundation (NI17-039), Azrieli Center for Autism Research (ACAR), and salary support from the Canada Research Chairs Program.

Data and code availability statement

Phenotypic and imaging data, as well as code for statistical analysis are freely available on our OSF repository: https://doi.org/10.17605/OSF.IO/JBDN2. For processing details, please see: https://github.com/rcruces/cognition_conectomics_TLE.

For additional details about all rCCA models, connectome parameterization, and the long table of ROIs of our segmentations, please see our OSF repository and supplementary material.

SurfStat is available via http://mica-mni.github.io/surfstat.

Declaration of competing interest

None.

CRediT authorship contribution statement

Raúl Rodríguez-Cruces: Conceptualization, Methodology, Software, Formal analysis, Investigation, Data curation, Writing - original draft. **Boris C. Bernhardt:** Conceptualization, Methodology, Writing - original draft. **Luis Concha:** Conceptualization, Investigation, Writing - original draft, Project administration, Funding acquisition.

Acknowledgements

We sincerely thank the patients and their families, as well as our control subjects, for their willingness to participate, the medical specialists who helped us with their recruitment, and the clinical personnel at the National Laboratory for magnetic resonance imaging. We are grateful to Juan Ortíz-Retana, Erick Pasaye and Leopoldo González-Santos for technical assistance. We extend our gratitude to the many people who have at some point participated in this study, performing patient recruitment, scanning, and clinical evaluations: Leticia Velázquez-Pérez, David Trejo, Héctor Barragán, Arturo Domínguez, Ildefonso Rodríguez-Leyva, Ana Luisa Velasco, Luis Octavio Jiménez, Daniel Atilano, Elizabeth González Olvera, Rafael Moreno, Vicente Camacho, Ana Elena Rosas, and Alfonso Fajardo.

Appendix A. Supplementary data

Supplementary data to this article can be found online at https://doi.org/10.1016/j.neuroimage.2020.116706.

References

Barron, D.S., Fox, P.T., Pardoe, H., Lancaster, J., Price, L.R., Blackmon, K., et al., 2015. Thalamic functional connectivity predicts seizure laterality in individual TLE patients: application of a biomarker development strategy. Neuroimage: Clin. 7, 273–280.

Bellec, P., Rosa-Neto, P., Lyttelton, O.C., Benali, H., Evans, A.C., 2010. Multi-level bootstrap analysis of stable clusters in resting-state fMRI. Neuroimage 51, 1126–1139. https://doi.org/10.1016/j.neuroimage.2010.02.082.

Bernhardt, B.C., Bernasconi, A., Liu, M., Hong, S.-J., Caldairou, B., Goubran, M., Guiot, M.C., Hall, J., Bernasconi, N., 2016. The spectrum of structural and functional imaging abnormalities in temporal lobe epilepsy. Ann. Neurol. 80, 142–153. https://doi.org/10.1002/ana.24691.

Bernhardt, B.C., Bernasconi, N., Concha, L., Bernasconi, A., 2010. Cortical thickness analysis in temporal lobe epilepsy: reproducibility and relation to outcome. Neurology 74, 1776–1784. https://doi.org/10.1212/WNL.0b013e3181e0f80a.

Bernhardt, B.C., Bonilha, L., Gross, D.W., 2015. Network analysis for a network disorder: the emerging role of graph theory in the study of epilepsy. Epilepsy Behav. 50, 162–170. https://doi.org/10.1016/j.yebeh.2015.06.005.

Bernhardt, B.C., Chen, Z., He, Y., Evans, A.C., Bernasconi, N., 2011. Graph-theoretical analysis reveals disrupted small-world organization of cortical thickness correlation networks in temporal lobe epilepsy. Cerebr. Cortex 21, 2147–2157. https://doi.org/10.1093/cercor/bhq291.

Bernhardt, B.C., Hong, S., Bernasconi, A., Bernasconi, N., 2013. Imaging structural and functional brain networks in temporal lobe epilepsy. Front. Hum. Neurosci. 7, 624. https://doi.org/10.3389/fnhum.2013.00624.

Bernhardt, B.C., Fadaie, F., Liu, M., Caldairou, B., Gu, S., Jefferies, E., et al., 2019. Temporal lobe epilepsy: hippocampal pathology modulates connectome topology and controllability. Neurology 92 (19), e2209–e2220.

Blanc, F., Martinian, L., Liagkouras, I., Catarino, C., Sisodiya, S.M., Thom, M., 2011. Investigation of widespread neocortical pathology associated with hippocampal sclerosis in epilepsy: a postmortem study. Epilepsia 52, 10–21. https://doi.org/10.1111/j.1528-1167.2010.02773.x.

Blümcke, I., Thom, M., Aronica, E., Armstrong, D.D., Bartolomei, F., Bernasconi, A., Bernasconi, N., Bien, C.G., Cendes, F., Coras, R., Cross, J.H., Jacques, T.S., Kahane, P., Mathern, G.W., Miyata, H., Moshé, S.L., Oz, B., Özkara, Ç., Perucca, E., Sisodiya, S., Spreafico, R., 2013. International consensus classification of hippocampal sclerosis in temporal lobe epilepsy: a Task Force report from the ILAE Commission on Diagnostic Methods. Epilepsia 54, 1315–1329. https://doi.org/10.1111/epi.12220.

Bonilha, L., Helpern, J.A., Sainju, R., Nesland, T., Edwards, J.C., Glazier, S.S., Tabesh, A., 2013. Presurgical connectome and postsurgical seizure control in temporal lobe epilepsy. Neurology 81, 1704–1710. https://doi.org/10.1212/01.wnl.0000435306.95271.5f.

Bonilha, L., Nesland, T., Martz, G.U., Joseph, J.E., Spampinato, M.V., Edwards, J.C., Tabesh, A., 2012. Medial temporal lobe epilepsy is associated with neuronal fibre loss and paradoxical increase in structural connectivity of limbic structures. J. Neurol. Neurosurg. Psychiatry 83, 903–909. https://doi.org/10.1136/jnnp-2012-302476.

Caciagli, L., et al., 2017. A meta-analysis on progressive atrophy in intractable temporal lobe epilepsy: Time is brain? Neurology 89 (5), 506–516. https://doi.org/10.1212/WNL.0000000000004176. In press.

Concha, L., Beaulieu, C., Gross, D.W., 2005. Bilateral limbic diffusion abnormalities in unilateral temporal lobe epilepsy. Ann. Neurol. 57, 188–196. https://doi.org/10.1002/ana.20334.

Coupé, P., Yger, P., Prima, S., Hellier, P., Kervrann, C., Barillot, C., 2008. An optimized blockwise nonlocal means denoising filter for 3-D magnetic resonance images. IEEE Trans. Med. Imag. 27 (4), 425–441.

Dabbs, K., Jones, J., Seidenberg, M., Hermann, B., 2009. Neuroanatomical correlates of cognitive phenotypes in temporal lobe epilepsy. Epilepsy Behav. 15, 445–451. https://doi.org/10.1016/j.yebeh.2009.05.012.

Diehl, B., Busch, R.M., Duncan, J.S., Piao, Z., Tkach, J., Lüders, H.O., 2008. Abnormalities in diffusion tensor imaging of the uncinate fasciculus relate to reduced memory in temporal lobe epilepsy. Epilepsia 49, 1409–1418. https://doi.org/10.1111/j.1528-1167.2008.01596.x.

Galovic, M., van Dooren, V.Q., Postma, T.S., Vos, S.B., Caciagli, L., Borzì, G., et al., 2019. Progressive cortical thinning in patients with focal epilepsy. JAMA Neurology 76 (10), 1230–1239.

Gleichgerrcht, Ezequiel, Kocher, Madison, Bonilha, Leonardo, 2015. Connectomics and graph theory analyses: novel insights into network abnormalities in epilepsy. Epilepsia 56 (11), 1660–1668.

González, I., Déjean, S., Martin, P.G., Baccini, A., Others, 2008. CCA: an R package to extend canonical correlation analysis. J. Stat. Software 23, 1–14. https://doi.org/10.18637/jss.v023.i12.

Hatton, S.N., Huynh, K.H., Bonilha, L., Abela, E., Alhusaini, S., Altmann, A.N., et al., 2019. White Matter Abnormalities across Different Epilepsy Syndromes in Adults: an ENIGMA Epilepsy Study (bioRxiv).

Helmstaedter, C., Elger, C.E., 2009. Chronic temporal lobe epilepsy: a neurodevelopmental or progressively dementing disease? Brain 132, 2822–2830. https://doi.org/10.1093/brain/awp182.

Hermann, B., Seidenberg, M., Lee, E.-J., Chan, F., Rutecki, P., 2007. Cognitive phenotypes in temporal lobe epilepsy. J. Int. Neuropsychol. Soc. 13, 12–20. https://doi.org/10.1017/S135561770707004X.

Honey, C.J., Sporns, O., Cammoun, L., Gigandet, X., Thiran, J.P., Meuli, R., Hagmann, P., 2009. Predicting human resting-state functional connectivity from structural connectivity. Proc. Natl. Acad. Sci. Unit. States Am. 106 (6), 2035–2040.

Hoppe, C., Elger, C.E., Helmstaedter, C., 2007. Long-term memory impairment in patients with focal epilepsy. Epilepsia 48 (Suppl. 9), 26–29. https://doi.org/10.1111/j.1528-1167.2007.01397.x.

Jones, D.K., Knösche, T.R., Turner, R., 2013. White matter integrity, fiber count, and other fallacies: the do's and don'ts of diffusion MRI. Neuroimage 73, 239–254.

Jeurissen, B., Leemans, A., Tournier, J.D., Jones, D.K., Sijbers, J., 2013. Investigating the prevalence of complex fiber configurations in white matter tissue with diffusion magnetic resonance imaging. Hum. Brain Mapp. 34 (11), 2747–2766. https://doi.org/10.1002/hbm.22099.

Khambhati, Ankit N., et al., 2016. Virtual cortical resection reveals push-pull network control preceding seizure evolution. Neuron 91 (5), 1170–1182.

Kebets, V., Holmes, A.J., Orban, C., Tang, S., Li, J., Sun, N., et al., 2019. Somatosensory-motor dysconnectivity spans multiple transdiagnostic dimensions of psychopathology. Biol. Psychiatr.

Kernbach, J.M., Yeo, B.T., Smallwood, J., Margulies, D.S., de Schotten, M.T., Walter, H., et al., 2018. Subspecialization within default mode nodes characterized in 10,000 UK Biobank participants. Proc. Natl. Acad. Sci. Unit. States Am. 115 (48), 12295–12300. https://doi.org/10.1073/pnas.1804876115.

Larivière, S., Weng, Y., de Wael, R.V., Frauscher, B., Wang, Z., Bernasconi, A., et al., 2019. Functional Connectome Contractions in Temporal Lobe Epilepsy, p. 756494 bioRxiv.

Lin, J.J., Mula, M., Hermann, B.P., 2012. Uncovering the neurobehavioural comorbidities of epilepsy over the lifespan. Lancet 380, 1180–1192. https://doi.org/10.1016/S0140-6736(12)61455-X.

Lin, J.J., Salamon, N., Lee, A.D., Dutton, R.A., Geaga, J.A., H Maier-Hein ayashi, K.M., Luders, E., Toga, A.W., Engel, J., Thompson, P.M., 2007. Reduced neocortical thickness and complexity mapped in mesial temporal lobe epilepsy with hippocampal sclerosis. Cerebr. Cortex 17, 2007–2018. https://doi.org/10.1093/cercor/bhl109.

Liu, M., Bernhardt, B.C., Bernasconi, A., Bernasconi, N., 2016. Gray matter structural compromise is equally distributed in left and right temporal lobe epilepsy. Hum. Brain Mapp. 37 (2), 515–524.

Maier-Hein, K.H., et al., 2017. The challenge of mapping the human connectome based on diffusion tractography. Nature comm. 8(1) (1349). https://doi.org/10.1038/s41467-017-01285-x. In press.

McDonald, C.R., Ahmadi, M.E., Hagler, D.J., Tecoma, E.S., Iragui, V.J., Gharapetian, L., Dale, A.M., Halgren, E., 2008. Diffusion tensor imaging correlates of memory and language impairments in temporal lobe epilepsy. Neurology 71, 1869–1876. https://doi.org/10.1212/01.wnl.0000327824.05348.3b.

McDonald, C.R., Leyden, K.M., Hagler, D.J., Kucukboyaci, N.E., Kemmotsu, N., Tecoma, E.S., Iragui, V.J., 2014. White matter microstructure complements morphometry for predicting verbal memory in epilepsy. Cortex 58, 139–150. https://doi.org/10.1016/j.cortex.2014.05.014.

McIntosh, A.R., Mišić, B., 2013. Multivariate statistical analyses for neuroimaging data. Annu. Rev. Psychol. 64, 499–525. https://doi.org/10.1146/annurev-psych-113011-143804.

Miller, K.L., Alfaro-Almagro, F., Bangerter, N.K., Thomas, D.L., Yacoub, E., Xu, J., et al., 2016. Multimodal population brain imaging in the UK Biobank prospective epidemiological study. Nat. Neurosci. 19 (11), 1523. https://doi.org/10.1038/nn.4393.

Mišić, B., Betzel, R.F., Nematzadeh, A., Goni, J., Griffa, A., Hagmann, P., et al., 2015. Cooperative and competitive spreading dynamics on the human connectome. Neuron 86 (6), 1518–1529.

Morgan, Victoria L., Abou-Khalil, Bassel, Rogers, Baxter P., 2015. Evolution of functional connectivity of brain networks and their dynamic interaction in temporal lobe epilepsy. Brain Connect. 5 (1), 35–44.

Niso, G., Carrasco, S., Gudín, M., Maestú, F., del-Pozo, F., Pereda, E., 2015. What graph theory actually tells us about resting state interictal MEG epileptic activity. Neuroimage: Clinical 8, 503–515.

Otte, W.M., van Eijsden, P., Sander, J.W., Duncan, J.S., Dijkhuizen, R.M., Braun, K.P.J., 2012. A meta-analysis of white matter changes in temporal lobe epilepsy as studied with diffusion tensor imaging. Epilepsia 53, 659–667. https://doi.org/10.1111/j.1528-1167.2012.03426.x.

Ponten, S.C., Bartolomei, F., Stam, C.J., 2007. Small-world networks and epilepsy: graph theoretical analysis of intracerebrally recorded mesial temporal lobe seizures. Clin. Neurophysiol. 118 (4), 918–927.

Qi, Shouliang, et al., 2015. The influence of construction methodology on structural brain network measures: a review. J. Neurosci. Methods 253, 170–182.

Raj, A., Mueller, S.G., Young, K., Laxer, K.D., Weiner, M., 2010. Network-level analysis of cortical thickness of the epileptic brain. Neuroimage 52, 1302–1313. https://doi.org/10.1016/j.neuroimage.2010.05.045.

Reyes, A., Kaestner, E., Bahrami, N., Balachandra, A., Hegde, M., Paul, B.M., Hermann, B., McDonald, C.R., 2019. Cognitive phenotypes in temporal lobe epilepsy are associated with distinct patterns of white matter network abnormalities. Neurology 92, e1957–e1968. https://doi.org/10.1212/WNL.0000000000007370.

Riley, J.D., Franklin, D.L., Choi, V., Kim, R.C., Binder, D.K., Cramer, S.C., Lin, J.J., 2010. Altered white matter integrity in temporal lobe epilepsy: association with cognitive and clinical profiles. Epilepsia 51, 536–545. https://doi.org/10.1111/j.1528-1167.2009.02508.x.

Rodríguez-Cruces, R., Concha, L., 2015. White matter in temporal lobe epilepsy: clinico-pathological correlates of water diffusion abnormalities. Quant. Imag. Med. Surg. 5, 264–278. https://doi.org/10.3978/j.issn.2223-4292.2015.02.06.

Rodríguez-Cruces, R., Velázquez-Pérez, L., Rodríguez-Leyva, I., Velasco, A.L., Trejo-Martínez, D., Barragán-Campos, H.M., Camacho-Téllez, V., Concha, L., 2018. Association of white matter diffusion characteristics and cognitive deficits in temporal lobe epilepsy. Epilepsy Behav. 79, 138–145. https://doi.org/10.1016/j.yebeh.2017.11.040.

Roine, T., Jeurissen, B., Perrone, D., Aelterman, J., Philips, W., Sijbers, J., Leemans, A., 2019. Reproducibility and intercorrelation of graph theoretical measures in structural brain connectivity networks. Med. Image Anal. 52, 56–67. https://doi.org/10.1016/j.media.2018.10.009.

Rubinov, M., Sporns, O., 2010. Complex network measures of brain connectivity: uses and interpretations. Neuroimage 52, 1059–1069. https://doi.org/10.1016/j.neuroimage.2009.10.003.

Schaefer, A., Kong, R., Gordon, E.M., Laumann, T.O., Zuo, X.N., Holmes, A.J., et al., 2017. Local-global parcellation of the human cerebral cortex from intrinsic functional connectivity MRI. Cerebr. Cortex 28 (9), 3095–3114. https://doi.org/10.1093/cercor/bhx179.

Seidenberg, M., Hermann, B., Pulsipher, D., Morton, J., Parrish, J., Geary, E., Guidotti, L., 2008. Thalamic atrophy and cognition in unilateral temporal lobe epilepsy. J. Int. Neuropsychol. Soc. 14 (3), 384–393.

Smith, R.E., Tournier, J.-D., Calamante, F., Connelly, A., 2012. Anatomically-constrained tractography: improved diffusion MRI streamlines tractography through effective use of anatomical information. Neuroimage 62, 1924–1938. https://doi.org/10.1016/j.neuroimage.2012.06.005.

Smith, R.E., Tournier, J.-D., Calamante, F., Connelly, A., 2013. SIFT: spherical-deconvolution informed filtering of tractograms. Neuroimage 67, 298–312. https://doi.org/10.1016/j.neuroimage.2012.11.049.

Smith, R.E., Tournier, J.-D., Calamante, F., Connelly, A., 2015a. The effects of SIFT on the reproducibility and biological accuracy of the structural connectome. Neuroimage 104, 253–265. https://doi.org/10.1016/j.neuroimage.2014.10.004.

Smith, S.M., Nichols, T.E., Vidaurre, D., Winkler, A.M., Behrens, T.E.J., Glasser, M.F., Ugurbil, K., Barch, D.M., Van Essen, D.C., Miller, K.L., 2015b. A positive-negative mode of population covariation links brain connectivity, demographics and behavior. Nat. Neurosci. 18, 1565–1567. https://doi.org/10.1038/nn.4125.

Tavakol, S., Royer, J., Lowe, A.J., Bonilha, L., Tracy, J.I., Jackson, G.D., et al., 2019. Neuroimaging and connectomics of drug-resistant epilepsy at multiple scales: from focal lesions to macroscale networks. Epilepsia 60 (4), 593–604.

Tracy, Joseph I., Doucet, Gaelle E., 2015. Resting-state functional connectivity in epilepsy: growing relevance for clinical decision making. Curr. Opin. Neurol. 28 (2), 158–165.

Tustison, N.J., Avants, B.B., Cook, P.A., Zheng, Y., Egan, A., Yushkevich, P.A., Gee, J.C., 2010. N4ITK: improved N3 bias correction. IEEE Trans. Med. Imag. 29 (6), 1310–1320. https://doi.org/10.1109/TMI.2010.2046908.

Vaessen, M.J., Jansen, J.F.A., Vlooswijk, M.C.G., Hofman, P.A.M., Majoie, H.J.M., Aldenkamp, A.P., Backes, W.H., 2012. White matter network abnormalities are associated with cognitive decline in chronic epilepsy. Cerebr. Cortex 22, 2139–2147. https://doi.org/10.1093/cercor/bhr298.

van Diessen, E., Diederen, S.J., Braun, K.P., Jansen, F.E., Stam, C.J., 2013. Functional and structural brain networks in epilepsy: what have we learned? Epilepsia 54 (11), 1855–1865.

Veraart, J., Novikov, D.S., Christiaens, D., Ades-Aron, B., Sijbers, J., Fieremans, E., 2016. Denoising of diffusion MRI using random matrix theory. Neuroimage 142, 394–406. https://doi.org/10.1016/j.neuroimage.2016.08.016.

Whelan, C.D., Altmann, A., Botía, J.A., Jahanshad, N., Hibar, D.P., Absil, J., Alhusaini, S., Alvim, M.K.M., Auvinen, P., Bartolini, E., Bergo, F.P.G., Bernardes, T., Blackmon, K.,

Braga, B., Caligiuri, M.E., Calvo, A., Carr, S.J., Chen, J., Chen, S., Cherubini, A., Sisodiya, S.M., 2018. Structural brain abnormalities in the common epilepsies assessed in a worldwide ENIGMA study. Brain 141, 391–408. https://doi.org/10.1093/brain/awx341.

Wieser, H.-G., Ilae Commission on Neurosurgery of Epilepsy, 2004. ILAE Commission Report. Mesial temporal lobe epilepsy with hippocampal sclerosis. Epilepsia 45, 695–714. https://doi.org/10.1111/j.0013-9580.2004.09004.x.

Worsley, K.J., Taylor, J.E., Carbonell, F., Chung, M.K., Duerden, E., Bernhardt, B., Lyttelton, O., Boucher, M., Evans, A.C., 2009. SurfStat: a Matlab toolbox for the statistical analysis of univariate and multivariate surface and volumetric data using linear mixed effects models and random field theory. Neuroimage 47, S102. https://doi.org/10.1016/S1053-8119(09)70882-1.

Yasuda, C.L., Chen, Z., Beltramini, G.C., Coan, A.C., Morita, M.E., Kubota, B., et al., 2015. Aberrant topological patterns of brain structural network in temporal lobe epilepsy. Epilepsia 56 (12), 1992–2002.

Yeh, C.-H., Smith, R.E., Liang, X., Calamante, F., Connelly, A., 2016. Correction for diffusion MRI fibre tracking biases: the consequences for structural connectomic metrics. Neuroimage 142, 150–162. https://doi.org/10.1016/j.neuroimage.2016.05.047.

Yeo, B.T., Krienen, F.M., Sepulcre, J., Sabuncu, M.R., Lashkari, D., Hollinshead, M., et al., 2011. The organization of the human cerebral cortex estimated by intrinsic functional connectivity. J. Neurophysiol. 106 (3), 1125–1165.